Electrical Power and Energy Systems 111 (2019) 58–65

Contents lists available at ScienceDirect

Electrical Power and Energy Systems

journal homepage: www.elsevier.com/locate/ijepes

Distributed voltage regulation of smart distribution networks: Consensus-based information synchronization and distributed model predictive control scheme

Yifei Guo[a,b], Qiuwei Wu[b,c,*], Houlei Gao[a], Feifan Shen[b]

[a] Key Laboratory of Power System Intelligent Dispatch and Control of Ministry of Education, Shandong University, China
[b] Centre for Electric Power and Energy, Department of Electrical Engineering, Technical University of Denmark, Lyngby 2800, Denmark
[c] School of Engineering and Applied Sciences, Harvard University, 29 Oxford Street, Cambridge, MA 02138, USA

ARTICLE INFO

Keywords:
Consensus protocol
Distributed generator (DG)
Distributed model predictive control (MPC)
Smart distribution network
Voltage control

ABSTRACT

This paper proposes a distributed voltage control (DVC) scheme for smart distribution networks with high penetration of inverter-based distributed generators (DGs), aiming to optimally coordinate DG units and on load tap changer (OLTC) transformer to regulate the voltages within the feasible range. The proposed scheme consists of two important parts: (1) distributed information synchronization (DIS) framework and (2) distributed model predictive control (DMPC)-based voltage control scheme. The DIS framework is established based on the consensus protocols to synchronize the specific information about the critical bus voltages and potential OLTC actions. The DMPC-based voltage control scheme is presented, in which each DG unit only exchanges information with its immediate neighbors and solves the local optimal control problem. Two control modes are designed to better deal with different operating conditions. In the normal mode, only the reactive power outputs of DG units are optimized to mitigate the voltage deviations. In the corrective mode, both of the active and reactive power outputs of DG units are optimally controlled to correct the severe voltage deviations. To mitigate the mutual interaction between the DGs and OLTC, the potential actions of OLTC are predicted and considered in the optimization problem of each units. The control performance of the proposed scheme was demonstrated using a real medium-voltage (MV) distribution network with two feeders under both normal and large-disturbance conditions.

1. Introduction

The integration of distributed generators (DGs) into power systems is worldwide encouraged by national policies to meet the rapidly increasing energy demand and alleviate the environmental problems [1,2]. Among the distributed energy resources available today, the inverter-based DGs such as solar photovoltaic and wind turbines are the most common form in medium-voltage (MV) and low-voltage distribution networks [3,4].

However, the increasing penetration of DG is challenging secure and stable operation of smart distribution networks. The voltage management problem is one of the main obstacles against installation of large amounts of DGs. The surplus power injections generated by DGs result in reverse power flow and hence voltage rise issue. Moreover, the stochastic and intermittent nature of renewable resources may cause significant voltage fluctuations. Generally, the distribution network operators regulate voltage profile across the network within an appropriate range using the conventional voltage regulation devices including on load tap changers (OLTCs), shunt capacitor banks and step voltage regulators, without considering the flexible and fast voltage regulation capability of DGs (normally operates with unity power factor), which cannot well control the voltage due to the slow response and discrete actions. Therefore, the voltage regulation of smart distribution networks has a prominent position in the research on smart grids, motivating a vast number of research work to tackle this problem [5]. The existing methods can be grouped into three categories, summarized as follows:

- **Local Control**. In the local voltage control schemes, the controllers receive the local information from the sensors surrounding them and perform control actions on their respective locality based on specific rules such as droop-based strategies [6–8], fuzzy logic-based methods [9] and sensitivity-based methods [10]. The local methods are easy to be implemented and do not require significant

* Corresponding author at: Centre for Electric Power and Energy, Department of Electrical Engineering, Technical University of Denmark, Lyngby 2800, Denmark.
E-mail addresses: qw@elektro.dtu.dk, qiuwu@seas.harvard.edu (Q. Wu).

https://doi.org/10.1016/j.ijepes.2019.03.059
Received 6 October 2018; Received in revised form 4 March 2019; Accepted 22 March 2019
Available online 09 April 2019
0142-0615/

investments of communication infrastructures compared with the communication-based ones. However, such a non-coordinated manner may result in negative interaction/hunting among the voltage regulation devices, posing the possibility of undesired islanding [11].

- **Centralized Control**. Due to the advancement in information and communication technologies, the centralized control schemes are attractive, which utilize the global information of the networks to achieve the coordination of multiple voltage regulation devices. Most of the centralized methods were designed by formulating the voltage control problems as the optimal power flow (OPF) models which minimize certain network-wide operation objectives including voltage deviations [12,14], power losses [13,14], number of OLTC actions [15], and curtailed energy [16,17], etc. Moreover, the centralized model predictive control (MPC)-based voltage control schemes were proposed in [17–19], which can effectively coordinate multiple DGs and the OLTC by introducing the prediction mechanism and hence shows good control performance. In [20], a combined centralized and local control scheme was proposed where the centralized controller designed based on the MPC modifies the V-Q characteristics of the local control. In [21], a two-tier voltage control scheme was proposed for distribution networks with electric springs (ESs) by combining the centralized and distributed control where the upper-level control is developed based on the MPC to regulate the OLTC and CBs.
- **Distributed Control**. The distributed voltage control schemes are widely developed based on the distributed control or distributed optimization techniques [5,22]. In [21], the lower-level control was designed to achieve responsibility sharing of ESs in a distributed manner using the consensus protocol. In [23], a two-stage distributed voltage control scheme was proposed, of which the first stage is the local control of each DG based on the sensitivity analysis and the second stage is developed to acquire reactive power support from other DGs. In [24], a consensus-based cooperative control scheme is proposed to regulate the voltages by coordinating the plug-in electric vehicles (PEVs) and active power curtailment of PV arrays. In [25], a distributed scheme that adjusts the reactive and active power output of PV inverters was proposed to prevent the over-voltage issues. In [26], a distributed coordinated control of energy storage systems was proposed for voltage regulation in distribution networks. In [27,28], the distributed voltage control schemes were established based on the multi-agent techniques with two-way communications. In [29–32], the optimal voltage control problems were formulated as an OPF model and solved in a distributed manner using the alternating direction method of multipliers algorithms. In [33], an optimal voltage control scheme was proposed based on the subgradient method. In [34], a consensus-based distributed intelligence algorithm was proposed to achieve the near-optimal loss minimization performance. The distributed control is more suitable for future networks with a large number of DGs due to its potential advantages in terms of computation burden, communication, response speed, plug-and-play capability, etc. [5,35,36].

The mutual interaction between distribution and transmission grids for voltage stability problems is also addressed. A case study to illustrate the interaction between transmission and active distribution networks was reported in [37]. A master-slave-splitting-based distributed global OPF method was presented in [38] considering transmission and distribution grids as a whole. And then in [39], a distributed voltage stability assessment method considering DGs is developed based on the distributed continuation power flow algorithm.

In this paper, a distributed voltage control (DVC) scheme for smart distribution networks with high penetration of inverter-based DGs is proposed to better regulate the voltage across the network. The proposed scheme includes two important parts: (1) distributed information synchronization (DIS) framework and (2) distributed MPC (DMPC)-based voltage control scheme. Compared with the existing works, the main contributions of this paper are threefold:

- A consensus-based DIS framework is proposed in this paper to synchronize the information including measured critical bus voltages and expected OLTC actions.
- The concept of DMPC is firstly used in voltage regulation of smart distribution networks with DGs, in which each DG unit only exchanges information with immediate neighboring DG units. Based on multi-step optimization, the proposed controller can smoothen system dynamics from the current state to the targeted state.
- The coordination between the OLTC with the distributed voltage control is addressed in this paper. The expected OLTC actions will be considered in the MPC formulation of each DG to avoid the mutual interaction with the OLTC.

The rest of this paper is organized as follows. Section 2 gives a brief overview of the proposed DVC. Section 3 presents the DIS framework. Section 4 presents the distributed MPC formulation of voltage control problem. Section 5 gives the coordination mechanism with the OLTC. Simulation results are presented and discussed in Section 6 followed by conclusions.

2. Overview of the proposed distributed voltage control scheme

The structure of the proposed DVC scheme is shown in Fig. 1. The scheme is divided into two parts: (1) the DIS framework and (2) the DMPC-based voltage control scheme. In the DIS framework, the operating information is synchronized (estimated by each DG) using the consensus protocols, including the critical bus voltages and accumulated time after the triggered signal of OLTC. Moreover, the information about reactive power outputs of neighboring DG units (include measured and predicted reactive power outputs) can be acquired by each DG as well. These necessary information will be used in the MPC. Note that, in Fig. 1, $j \in \mathcal{N}_i$ denotes there is communication between Unit i and Unit j. The DIS framework design is described in Section 3 in detail. In the second part, the DMPC controller formulates the voltage control problem as a multi-step constrained optimization model and then solves it to obtain the power references of DGs.

The voltage sensitivities with respect to power injections $\partial V/\partial P$, $\partial V/\partial Q$ and $\Delta V/\Delta N_{tap}$ tap changes are related to the operating point and network parameters. However, the global information could not be available for distributed controllers. According to the numerical analysis, the sensitivities vary within very limited range during the steady state operation. Therefore, the voltage sensitivities are calculated offline based on an analytical sensitivity calculation method [40]. It is expected that the closed-loop nature of MPC will compensate the minor errors of sensitivity coefficients.

Two control modes, namely *normal mode* and *corrective mode*, are designed in this scheme which are determined by the voltage conditions. In the *normal mode*, the DG units operate at the maximum power

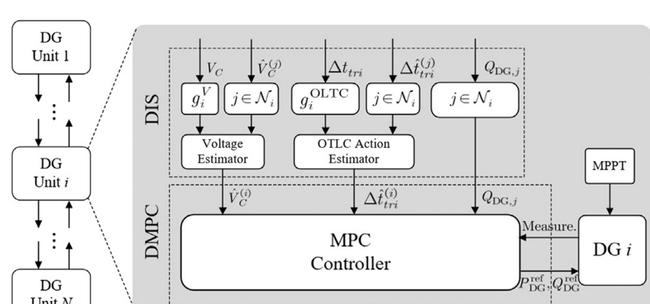

Fig. 1. Structure of the proposed distributed voltage control scheme.

point tracking (MPPT) mode to capture more energy. The MPC controller only optimally controls the reactive power outputs of DG inverters to correct voltage deviations. In the *corrective mode*, in addition to reactive power support, necessary active power curtailment of DG units is also used to correct the severe voltage deviations. The details can be found in Section 4.

In this paper, the proposed distributed control scheme is only investigated from the technical perspective. However, the DGs are generally owned by customers instead of the DNOs. Therefore, the economic compensation issues should be addressed for a practical implementation since additional reactive power injections can result in power loss inside the inverters and may accelerate the degradation of the inverters. Economic incentives via a marketing mechanism should be clarified to encourage the DG owners to provide voltage support service for distribution networks [41–44].

3. Consensus-based distributed information synchronization

3.1. Preliminaries

3.1.1. Graph theory

Let $\mathcal{G} = (\mathcal{V}, \mathcal{E}, \mathcal{A})$ be a weighted undirected graph with the vertex set $\mathcal{V} = \{v_1, v_2, ..., v_N\}$, edge set $\mathcal{E} \subseteq \mathcal{V} \times \mathcal{V}$ and adjacency matrix $\mathcal{A} = [a_{ij}]$. The vertex indexes belong to a finite set $\mathcal{I} = \{1, 2, ..., N\}$. An edge of $\mathcal{G}$ is denoted by $e_{ij} = (v_i, v_j)$. The adjacency elements associated with the edges of the graph are positive, i.e., $e_{ij} \in \mathcal{E} \Leftrightarrow a_{ij} > 0$ and assume $a_{ii} = 0$. The set of neighbors of node v_i is denoted by $\mathcal{N}_i = \{j \in \mathcal{V} | (v_i, v_j) \in \mathcal{E}\}$. The Laplacian matrix of the graph is defined as $\mathcal{L} = \mathcal{D} - \mathcal{A}$ where $\mathcal{D} = \mathrm{diag}(d_1, d_2, \cdots, d_N)$ is the diagonal matrix with $d_i = \sum_{j \in \mathcal{N}_i} a_{ij}$ denoting the degree matrix.

3.1.2. Consensus protocols on graphs

Let $x_i \in \mathbb{R}$ denotes the value of node v_i (agent *i*). Let $\mathcal{M}: \mathbb{R}^N \to \mathbb{R}$ be a function of N variables $x_1, x_2 ... x_N$ and $x_1(0), x_2(0) ... x_N(0)$ denote the initial state of the system. The $\mathcal{M}$-consensus problem is to calculate $\mathcal{M}(x_1(0), x_2(0) ... x_N(0))$ in a distributed manner by applying the inputs (state feedback) u_i, of which the discrete model of the dynamics of each node v_i in the consensus protocols can be described as [45],

$$x_i(k+1) = f(x_i(k), u_i(k)), \quad i \in \mathcal{I} \tag{1a}$$

$$u_i(k) = g(x_i(k), (x_{j_1}(k), x_{j_2}(k), ..., x_{j_{n_i}}(k))) \tag{1b}$$

where the indexes $j_1, j_2, ..., j_{n_i} \in \mathcal{N}_i$; $f(\cdot)$ and $g(\cdot)$ denote the rules to solve different consensus problems. The protocols solve the $\mathcal{M}$-consensus problems if and only if there exists a asymptotically stable equilibrium x^*, which satisfies $x_1(\infty) = x_2(\infty) = \cdots = x_N(\infty) = x^*$.

In this paper, x_i represents the voltage and accumulated triggered time of the OLTC, which will be synchronized using different consensus protocols (average-consensus and max-consensus, respectively).

3.1.3. Leaders and followers

The agents (DG units) are divided into two categories in the protocols. The DG units having direct access to the reference information are defined as leaders, otherwise, defined as followers. To save the communication investment (nearby principle), it is worth noting that being leader or follower for one unit is not rigid, i.e., one unit may have different roles in different information synchronization problems. The leader and follower sets are denoted by $\mathcal{L}^{(\cdot)}$ and $\mathcal{F}^{(\cdot)}$, respectively.

The schematic diagram of the distributed information synchronization framework is shown in Fig. 2. In this figure, Unit 1 and Unit 4 are the leaders in terms of synchronization of information x and y, respectively.

3.2. Synchronization of monitored bus voltages

The monitored bus voltages sent to the neighboring units that are

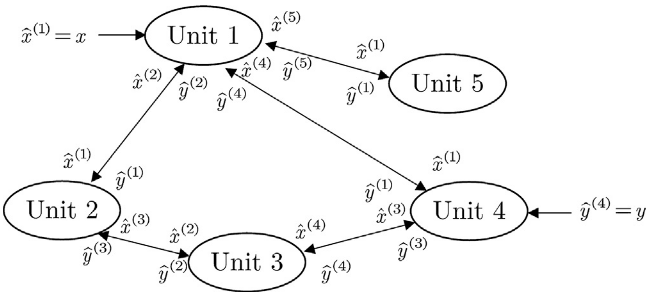

Fig. 2. Distributed information synchronization/estimation framework (x and y denote the information which is required to be synchronized; and $\hat{x}^{(i)}$ and $\hat{y}^{(i)}$ denote the estimated values at Unit *i*).

regarded as the leaders. The voltages of monitored buses are synchronized by using the average-consensus protocol, of which the discrete model is,

$$\hat{V}_C^{(i)}(k+1) = \begin{cases} V_C, \forall i \in \mathcal{L}^V, \\ \hat{V}_C^{(i)}(k) + \mu_i \sum_{j=1}^{N} a_{ij}(\hat{V}_C^{(j)}(k) - \hat{V}_C^{(i)}(k)), \\ \forall i \in \mathcal{F}^V, \end{cases} \tag{2}$$

where $\hat{V}_C^{(i)}$ and $\hat{V}_C^{(j)}$ denote the monitored bus voltage estimated by Unit *i* and Unit *j*, respectively; V_C is the measured voltage magnitude; $\mu_i^V > 0$ denote the constant gain. The gains a_{ij} depend on the information that Unit *i* can receive. Since the process (2) can converge to V_C, each DG can estimate the monitored bus voltages which will be used for the DMPC.

3.3. Synchronization of triggered information of the OLTC

Similarly, the triggered information of the OLTC is sent to the neighboring DG units. Here, to realize the distributed information synchronization based on the consensus protocol, the accumulated time interval after the triggered signal (stops after the tap operation is finished) Δt_{tri} is synchronized rather than the triggered time using the max-consensus protocol. Each unit updates the information according to,

$$\Delta\hat{t}_{\mathrm{tri}}^{(i)}(k+1) = \begin{cases} \Delta t_{\mathrm{tri}}, \ \forall i \in \mathcal{L}^{\mathrm{OLTC}}, \\ \max\{\Delta\hat{t}_{\mathrm{tri}}^{(j)}(k)\}, \ \forall i \in \mathcal{F}^{\mathrm{OLTC}}, j \in \mathcal{N}_i \end{cases} \tag{3}$$

where $\Delta\hat{t}_{\mathrm{tri}}^{(i)}$ is the accumulated time estimated by Unit *i*. It is worth noting that $\Delta\hat{t}_{\mathrm{tri}}^{(i)}$ will be reset to "0" after each control point.

Note that, in the DIS framework, the information exchange among agents is performed all the time with much faster update rate than the DMPC framework (20 ms vs. 500 ms in this case). This decouples the DIS with the DMPC in terms of time scale to avoid the instability caused by the interaction between the DIS and DMPC. The fast convergence of the DIS can be guaranteed by selecting large gains. There is a possibility that the DIS does not perfectly converge when the DMPC is activated. It is expected that the closed-loop nature of MPC can compensate the inaccuracy.

4. Distributed model predictive control scheme

MPC has been successfully used in the voltage control which offers several appealing features such as handling multivariable control problems, ease of tuning and explicit consideration of constraints [5]. In the MPC, the control commands are obtained by solving a discrete-time optimal control problem over a given horizon, which is formulated based on the real-time measurements. An optimal control command sequence is produced and only the first control in the sequence is applied. The MPC can smoothen the system dynamics from the current state to the targeted state due to the multi-step optimization. Besides, the closed-loop nature of MPC can effectively account for the model inaccuracy, failure or delays of the control actions [17].

4.1. Modeling

4.1.1. DG

For the inverter-based DG, its control system typically consists two cascading control loops, i.e., the outer voltage loop and inner current loop, resulting in fast and continuous output power regulation capability. The fast dynamics can be neglected, i.e.,

$$P_{DG} = P_{DG}^{ref} \text{ and } Q_{DG} = Q_{DG}^{ref} \tag{4}$$

since the network-level control is generally designed to be decoupled with the DG's own control system in terms of time scale so as to avoid the instability issue. The power outputs of DG units are limited by,

$$0 \leqslant P_{DG} \leqslant \overline{P}_{DG} \tag{5a}$$

$$\sqrt{P_{DG}^2 + Q_{DG}^2} \leqslant S_{DG} \tag{5b}$$

$$\Delta \underline{Q}_{DG} \leqslant \Delta Q_{DG} \leqslant \Delta \overline{Q}_{DG} \tag{5c}$$

where $\overline{P}_{DG}$ is the maximum available power of DG, S_{DG} is the rated capacity of the inverter, and $\Delta \overline{Q}_{DG}$ is its maximum reactive power ramping limit.

4.1.2. Network voltage

In the MPC, the network voltage is predicted based on the first-order approximation model which is obtained by linearizing the network model around the operating point using the sensitivity coefficients, i.e.,

$$V = V(0) + \frac{\partial V}{\partial u}\Delta u \tag{6}$$

where u and Δu denote the control variables including the power injections of DGs and tap changes and its increment, respectively. This linearized model has been widely used in the MPC. The MPC problem by formulated as a standard convex constrained QP problem and can be efficiently solved. It is expected that the minor errors of the linearized model can be compensated by closed-loop nature of MPC.

4.2. DMPC formulation

The communication-based DMPC is adopted in this paper. At each control step, each unit receives information about the control commands executed by their neighboring units in the previous time step and other necessary updated state information. Then, an optimization problem only with the local cost function is solved where the interaction among the neighboring units is considered. If the communication-based iterations converge, a Nash equilibrium is achieved [46,47].

Suppose the prediction and control horizon (steps) are H_p ($N_p = H_p/T_c$) and H_c ($N_c = H_c/T_c$), respectively. As known, $N_p \geqslant N_c$. From the computational viewpoint, they should be equal unless the controller is required to consider changes beyond the control horizon, i.e. $N_p = N_c$ [17].

Firstly, to clearly present the DMPC formulation, the following definitions are provided. Define the measurements of active and reactive power of DG units at step k as,

$$\mathbf{P}(k) := [P_{DG,1}(k), \ldots, P_{DG,N_{DG}}(k)]^T,$$
$$\mathbf{Q}(k) := [Q_{DG,1}(k), \ldots, Q_{DG,N_{DG}}(k)]^T.$$

Define the predicted trajectory vectors of active power, reactive power and reactive power utilization ratio of DG units at step $k + l$ ($l = 1, \ldots, N_p$) estimated at step k, as,

$$\hat{\mathbf{P}}(k+l|k) := [P_{DG,1}(k+l|k), \ldots, P_{DG,N_{DG}}(k+l|k)]^T,$$
$$\hat{\mathbf{Q}}(k+l|k) := [Q_{DG,1}(k+l|k), \ldots, Q_{DG,N_{DG}}(k+l|k)]^T.$$

Define the vectors of predicted monitored bus voltages and voltage sensitivity of monitored bus $i \in \mathcal{B}_C$ where $\mathcal{B}_C$ denotes the set of monitored buses, with respect to active and reactive power injections by,

$$\mathbf{S}_i^P := \left[\frac{\partial V_{C,i}}{\partial P_{DG,1}}, \ldots, \frac{\partial V_{C,i}}{\partial P_{DG,N_{DG}}}\right]^T, \; i \in \mathcal{B}_C$$
$$\mathbf{S}_i^Q := \left[\frac{\partial V_{C,i}}{\partial Q_{DG,1}}, \ldots, \frac{\partial V_{C,i}}{\partial Q_{DG,N_{DG}}}\right]^T, \; i \in \mathcal{B}_C.$$

4.2.1. Normal mode

If all monitored bus voltages are within the predefined limits $[V_{ref} - V_{th}, V_{ref} + V_{th}]$, the controller will be in the normal mode, where V_{th} denotes the threshold which is typically $V_{DB}/2$ (the predefined deadband of the OLTC, see Section 5) for the MV bus and [0.05, 0.08] p.u. for others. V_{ref} denotes the voltage reference which is typically set as 1.0 p.u.. Based on this design, the OLTC will not participate in the voltage control in this mode.

In this mode, the MPC controller aims to regulate the voltage within a predefined range while keeping the fair reactive power sharing (identical reactive power utilization). Suppose the current time step is k (at the control point), the optimal control problem of DG i can be formulated as,

$$J_1 = W_V \sum_{l=1}^{N_p} \sum_{j \in \mathcal{B}_C} (\Delta \hat{V}_{C,j}(k+l|k) + \varepsilon(\hat{V}_{C,j}^{(i)} - V_{ref}))^2 + W_Q \sum_{l=1}^{N_p} (Q_{DG,i}(k+l|k) - Q_{DG,i}(k+l-1|k)) \tag{7}$$

$$\underset{Q_{DG,i}(k), \ldots, Q_{DG,i}(k+N_p-1)}{\text{minimize}} \quad J_1 \tag{8a}$$

subject to

$$\Delta \hat{V}_{C,j}\left(k + l \middle| k\right) = \frac{\partial V_{C,j}}{\partial Q_{DG,i}}(Q_{DG,i}(k+l|k) - Q_{DG,i}(k)) + (\mathbf{S}_j^Q)^T((\hat{\mathbf{Q}}(k+l|k-1) - \mathbf{Q}(k)) \odot \mathcal{A}_i) \tag{8b}$$

$$\underline{Q}_{DG,i} \leqslant Q_{DG,i}(k+l|k) \leqslant \overline{Q}_{DG,i} \tag{8c}$$

$$\Delta \underline{Q}_{DG,i} \leqslant \Delta Q_{DG,i}(k+l|k) \leqslant \Delta \overline{Q}_{DG,i} \tag{8d}$$

where the first term in the cost function J_1 is used to mitigate the voltage deviations, the second term is used to achieve fair reactive power sharing among DGs and the third term is to smoothen the reactive power variations. W_V, W_α and W_Q denote the corresponding weighting factors. The constant gain ε is used to adjust the control performance and guarantee the closed-loop stability. $\odot$ denotes the element-wise multiplication, $\mathcal{A}_i$ denotes the ith column of matrix $\mathcal{A}$ and the corresponding term represents the effect of immediate neighbors which can exchange information with DG unit i.

4.2.2. Corrective mode

If any monitored bus voltage violates the predefined limit, the MPC controller will switch to the corrective mode. In this mode, both the active and reactive power outputs of DG units are optimized to correct the severe voltage deviations while minimizing the curtailed power. Thus, the control problem can be formulated as,

$$J_2 = W_V \sum_{l=1}^{N_p} \sum_{j \in \mathcal{B}_C} (\Delta \hat{V}_{C,j}(k+l|k) + \varepsilon(\hat{V}_{C,j}^{(i)} - V_{ref}))^2 + W_P \sum_{l=1}^{N_p} (P_{DG,i}(k+l|k) - \overline{P}_{DG,i})^2 \tag{9}$$

$$\underset{P_{DG,i}(k),\ldots,P_{DG,i}(k+N_p-1),Q_{DG,i}(k),\ldots,Q_{DG,i}(k+N_p-1)}{\text{minimize}} \quad J_2 \tag{10a}$$

subject to

$$\Delta\widehat{V}_{C,j}\left(k+l\middle|k\right) = \frac{\partial V_{C,j}}{\partial P_{DG,i}}(P_{DG,i}(k+l|k) - P_{DG,i}(k))$$
$$+\frac{\partial V_{C,j}}{\partial Q_{DG,i}}(Q_{DG,i}(k+l|k) - Q_{DG,i}(k))$$
$$+(\mathbf{S}_j^P)^T((\widehat{\mathbf{P}}(k+l|k-1) - \mathbf{P}(k)) \odot \mathcal{A}_i)$$
$$+(\mathbf{S}_j^Q)^T((\widehat{\mathbf{Q}}(k+l|k-1) - \mathbf{Q}(k)) \odot \mathcal{A}_i)$$
$$+\text{Sign}_{tap}\left(k+l\right)\cdot\frac{\partial V_{C,j}}{\partial N_{tap}}\cdot\Delta N_{tap} \tag{10b}$$

$$0 \leqslant P_{DG,i}(k+l|k) \leqslant \overline{P}_{DG,i} \tag{10c}$$

$$\underline{Q}_{DG,i} \leqslant Q_{DG,i}(k+l|k) \leqslant \overline{Q}_{DG,i} \tag{10d}$$

$$\Delta\underline{Q}_{DG,i} \leqslant \Delta Q_{DG,i}(k+l|k) \leqslant \Delta\overline{Q}_{DG,i} \tag{10e}$$

where the first term in the cost function is used to penalize the voltage deviations and the second term is to minimize the curtailed energy of DGs where W_P denotes the weighting factor for active power curtailment. Sign_{tap} denotes if there is a potential tap change within the step $k+l$. When solving the problem, the reactive power limit is firstly considered as the rated capacity of the inverter. If the solution exceed the rated capacity limit, the closest point within the limit is selected as the solution. The potential OLTC action is considered in this mode which is predicted based on the method presented in Section 5.

The presented MPC problem can be transformed into a standard quadratic programming problem and can be efficiently solved in milliseconds by the commercial solvers.

5. Coordination with OLTC

The OLTC is an efficient voltage control device which can directly change the voltage level of the whole distribution network. The OLTC is controlled in a local manner instead of being optimized together with DGs. The reasons are as follows:

- The DMPC scheme is designed in a much faster time scale than the mechanical time delay of OLTC actions, which is generally in several seconds. The OLTC actions cannot be finished during one control period.
- In this scheme, it just needs time information sent from the OLTC controller rather than changing the existing control structure of OLTC, implying less extra investment.
- It could avoid more computation complexity due to the introduction of discrete control variables, which can result in a mix-integer nonlinear programming problem.

The principle of OLTC operation is illustrated in Fig. 3. The OLTC will perform a tap change if the controlled bus voltage violates the predefined deadband V_{DB} for longer than a predefine time delay T_{delay}. V_{DB} and T_{delay} are introduced in order to avoid frequent and unnecessary switching around the reference voltage V_{MV}^{ref}, which may result in the reduction of OLTC lifetime. V_{DB} is often designed symmetrical around the reference. The mechanical time delay T_{mech}, typically in $3 \sim 10$ s, is required for the OLTC to move the taps by one position. The non-sequential mode is adopted for the OLTC, in which the OLTC makes no distinction between the first and subsequent tap changes. Thus, suppose the estimated accumulated time is $\Delta\widehat{t}_{tri}$, the time of the tap change can be estimated as $\widehat{t}_{act} = t_0 - \Delta\widehat{t}_{tri} + T_{mech}$.

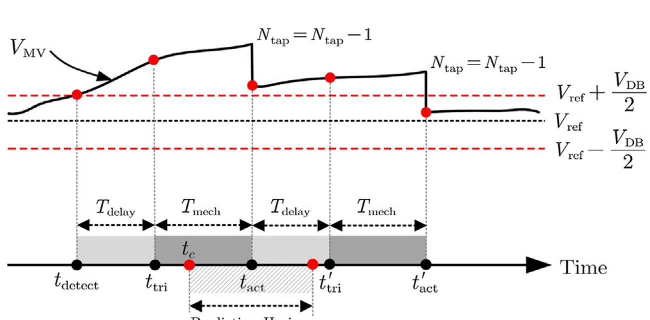

Fig. 3. The principle of OLTC operation.

In this paper, the voltage of the MV side bus of the main transformer V_{MV} is controlled by the OLTC. At each control point, if the tap action has been triggered and the current tap position is not at the minimum $\underline{N}_{tap}$ (for $V_{MV} > V_{ref} + V_{DB}/2$) or maximum position $\overline{N}_{tap}$ (for $V_{MV} < V_{ref} - V_{DB}/2$), Δt_{tri} will be sent to the closest agents (if not, $\Delta t_{tri} = 0$ will be sent). Then, each MPC controller will detect if there is a potential tap change within the prediction horizon. Suppose the current time is t_0, the indication of the potential tap change for the kth prediction step $\text{Sign}_{tap}(k)$ can be obtained by,

$$\text{Sign}_{tap}(k) = \begin{cases} 1, \text{ if } t_0 < \widehat{t}_{act} \leqslant t_0 + k \times T_c \\ 0, \text{ otherwise.} \end{cases} \tag{10f}$$

6. Case study

In this section, the control performance of the proposed DVC is demonstrated by using a real Finnish distribution network consisting of two 20 kV feeders [13]. The network topology as well as the communication network topology is presented in Fig. 4 and the corresponding adjacent matrix is,

$$\mathcal{A} = \begin{bmatrix} 0&1&0&0&1&0&0&0&0&0 \\ 1&0&1&0&0&0&0&0&0&0 \\ 0&1&0&1&0&0&0&0&0&0 \\ 0&0&1&0&0&0&0&0&0&1 \\ 1&0&0&0&0&1&0&0&0&0 \\ 0&0&0&0&1&0&1&0&0&0 \\ 0&0&0&0&0&1&0&1&0&0 \\ 0&0&0&0&0&0&1&0&1&0 \\ 0&0&0&0&0&0&0&1&0&1 \\ 0&0&0&1&0&0&0&0&1&0 \end{bmatrix}. \tag{10g}$$

This means if $a_{ij} = 1$, then Unit i and Unit j can exchange

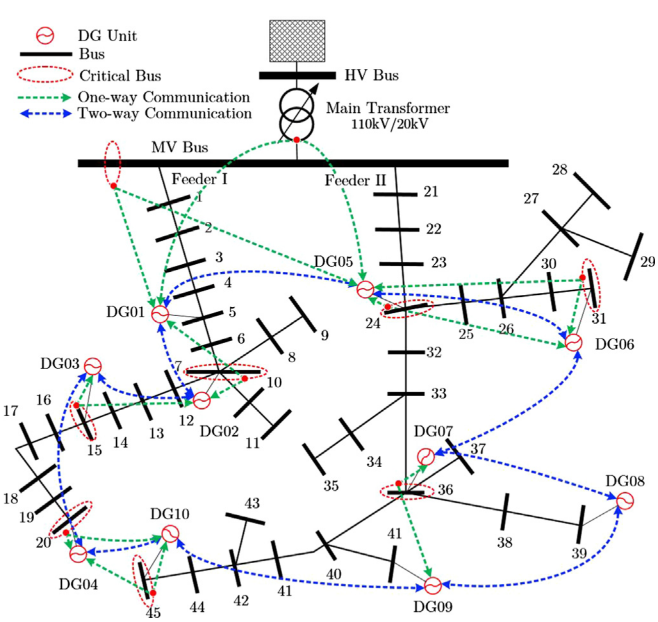

Fig. 4. Network topology of the test system.

Table 1
Leaders in the DIS framework.

Information	Leader
OLTC Info. (Δt_{tri})	DG01, DG05
Bus voltage (V_{MV})	DG01, DG05
Bus voltage (V_{Bus07})	DG01, DG02
Bus voltage (V_{Bus15})	DG02, DG03
Bus voltage (V_{Bus20})	DG04, DG10
Bus voltage (V_{Bus24})	DG05, DG06
Bus voltage (V_{Bus31})	DG05, DG06
Bus voltage (V_{Bus36})	DG07, DG09
Bus voltage (V_{Bus45})	DG09, DG10

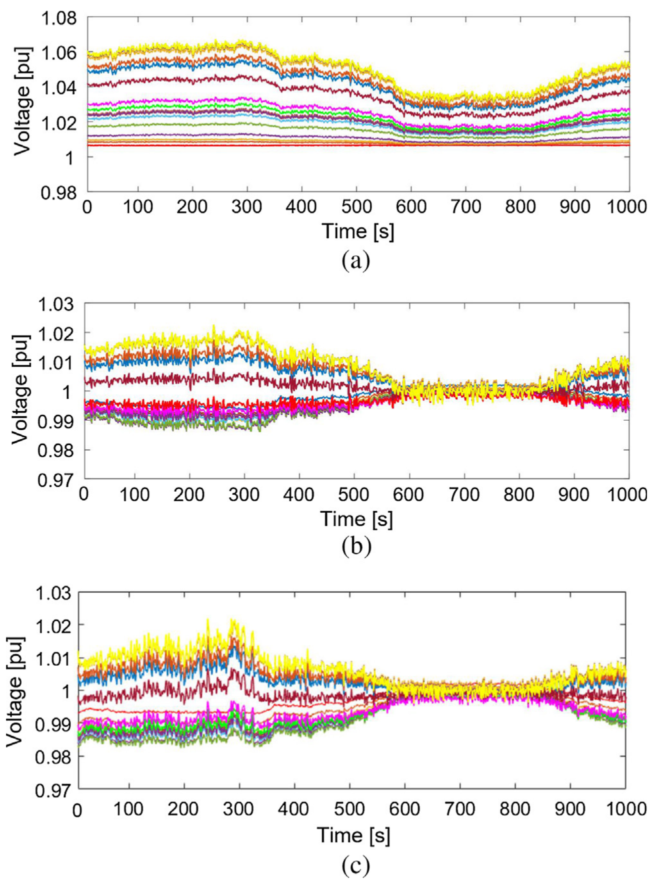

Fig. 5. Voltage profile of Feeder I with the different control schemes (Different colors represent different bus voltages). (a) PFC, (b) CMPC, and (c) DMPC. (For interpretation of the references to colour in this figure legend, the reader is referred to the web version of this article.)

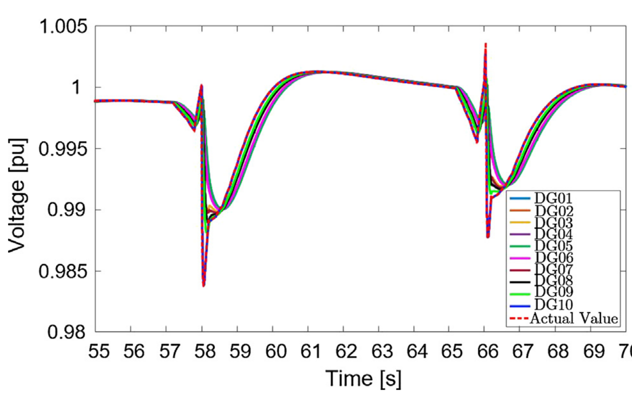

Fig. 6. Synchronization of V_{Bus20} (average-consensus).

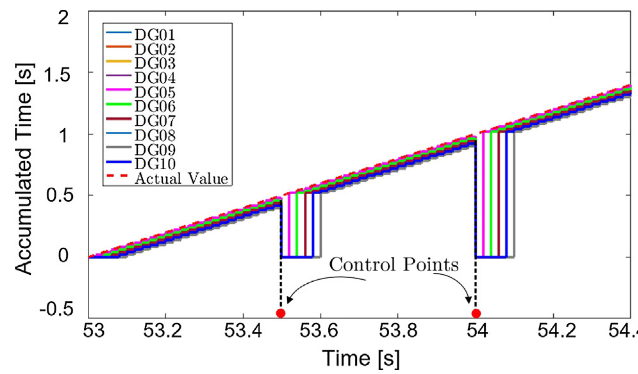

Fig. 7. Synchronization of Δt_{tri} (max-consensus).

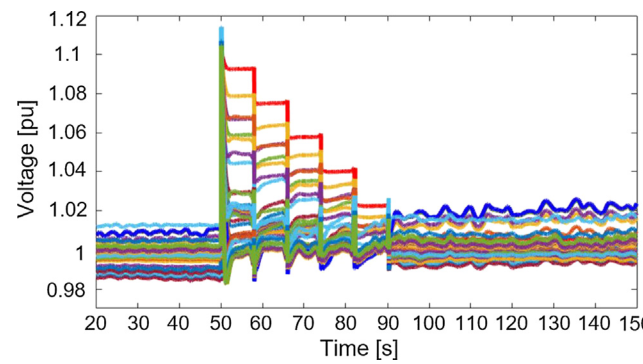

Fig. 8. Voltage profile across the network with the DMPC.

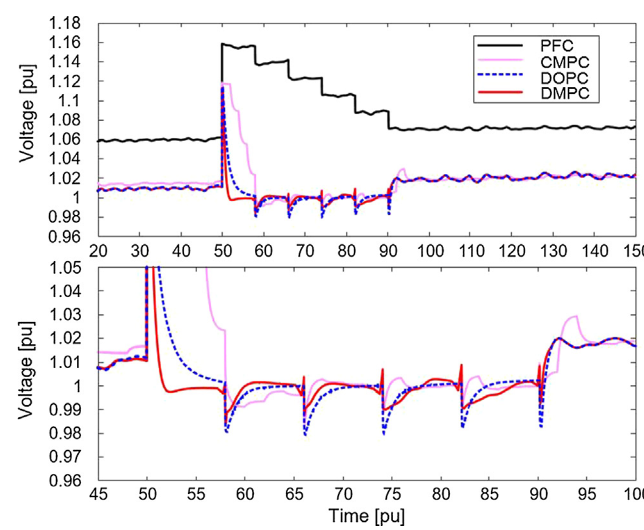

Fig. 9. Comparison of voltages of Bus 20 under emergency operation with the PFC, CMPC, DOPC and DMPC.

information using the two-way communication. As shown in Fig. 4, 10×1 MW inverter-based DG units (DG 01~DG 10) are placed at Bus 05, 07, 15, 20, 24, 31, 36, 39, 41 and 45, respectively. Each DG is equipped with a smart agent which can send/receive information and solve the control problems. In order to guarantee the robustness of the DIS, the accumulated time of the OLTC is sent to DG 01 and DG 05, respectively and the measurements of monitored bus voltages are sent to the closest two DG units using the one-way communications. According to [48], the minimum information update interval in IEEE 802.11 (Wi-Fi) is of the order of 10 ms, which is adequate for the DIS system. Therefore, the information update rate of the DIS is set as 20 ms. The details of the leaders in the DIS framework for each targeted information is listed in Table 1. The deadband V_{DB} and predefined time delay T_{delay} are set as 4% and 3 s. The tap changing range of the OLTC is $\pm 9 \times 1.67\%$ and the mechanical delay is 5 s. The threshold for other buses V_{th} is set as 0.05 p. u.. Based on the radial topology of the network, Buses 07, 15, 20, 24, 31, 36, 45 and the MV side bus of the main transformer are selected as the monitored buses.

In order to have stable operation, the network control has to be slowed down to have at least 5–10 times lower bandwidth than the DG units. Thus, the control period of the DMPC controllers is designed as 0.5 s. The prediction and control steps are designed as $N_p = N_c = 5$.

6.1. Normal operation

In this subsection, the control performance of the proposed DVC (DMPC) under normal operation is presented and compared with the conventional local constant power factor control (PFC) and centralized MPC (CMPC). Considering the negligible communication delay and solution time of the centralized control methods, the control period of the CMPC is designed as 2 s. Dynamic voltage profiles of Feeder I are shown in the Fig. 5. As can be seen from Fig. 5(a), the local PFC fails to regulate the voltages within the predefined range of [0.95, 1.05] p. u.. However, the CMPC and DMPC can both effectively regulate the voltages within the range of [0.98, 1.02] p. u., implying the CMPC and DMPC have the similar control performances under normal operation. Moreover, the results can verify that the network voltage profile can be well regulated only based on several monitored voltage bus instead of all bus voltage measurements and feedback in the network. This would be helpful to reduce the communication and computation burdens of the system.

6.2. Large-disturbance operation

In this subsection, the control performance under large disturbances in the external grid is examined and compared with the PFC, CMPC and the conventional one-step optimization-based distributed optimal control (DOPC) without prediction mechanism, of which the control period is designed as 0.5 s. At $t = 50$ s, the distribution network is affected by a significant disturbance in the external grid, namely a sudden step increase of slack bus voltage (at the HV side of the main transformer).

6.2.1. Information synchronization performance

The synchronization procedures of the voltage of Bus 20 (monitored bus) V_{Bus20} and the accumulated time Δt_{tri} are illustrated in Figs. 6 and 7, respectively. As can be seen, the DIS system can fast track the synchronized information of monitored bus voltages and OLTC actions, providing accurate data feedback for the MPC controller. This validates the effectiveness of the propose DIS framework. In Fig. 7, the solid lines represent the accumulated time estimated by DG01-DG08, respectively. The dash line represents its actual value. And to be noticed, it is reset to "0" after each control point of the DMPC controller (such as $t = 53.5$ s and $t = 54$ s). This effectively validates the max-consensus protocol designed in (3).

6.2.2. Voltage regulation performance

The voltage performances under the emergency operation are illustrated in Figs. 8 and 9. Firstly, as can be seen from Fig. 8, after the disturbance at $t = 50$ s, the network voltages violate the predefined range and go beyond 1.1 p. u.. Then, the OLTC and DVC can cooperatively correct the severe voltage deviations within the feasible range [0.98, 1.02] p. u. until $t = 90$ s.

As shown in Fig. 9, the optimal control methods, i.e., the CMPC, DOPC and DMPC, can effectively accelerate the voltage recovery. Comparably, the DMPC can help voltages recover much faster.

7. Conclusion

This paper proposes a DVC scheme for smart distribution networks with inverter-based DGs to regulate the voltage across the network within the feasible range. The proposed scheme includes two parts: the DIS framework and DMPC-based voltage control scheme. The former is developed using the consensus protocol to synchronize the monitored bus voltages and triggered time information of the OLTC. The synchronization performance has been proven to be effective and fast enough. Simulation results validate the effectiveness of the proposed DVC. Under normal operation, it can effectively regulate the voltages within the feasible range. Under large-disturbance conditions, it is also able to correct the voltage deviations and avoid the hunting between the DGs and OLTC. Compared with the PFC, CMPC and DOPC, it can better accelerate and smoothen the voltage recovery. The distributed control is suitable due to its good scalability and flexibility for the future smart distribution networks with a large number of DGs.

Acknowledgment

This work is supported in part by the ForskEL program through the 'IDE4L-DK Top-Up' project, in part by the National Key Research and Development Program of China (2016YFB0900603), in part by National Natural Science Foundation of China under grant 51877127, and in part by the China Scholarship Council (CSC).

References

[1] Tan J, Wang L. A game-theoretic framework for vehicle-to-grid frequency regulation considering smart charging mechanism. IEEE Trans Smart Grid 2017;8(5):2358–69.
[2] Yang H, Li S, Li Q, et al. Hierarchical distributed control for decentralized battery energy storage system based on consensus algorithm with pinning node. Protect Control Modern Power Syst 2018;3(1):1–9.
[3] Alam MJE, Muttaqi KM, Sutanto D. Mitigation of rooftop solar PV impacts and evening peak support by managing available capacity of distributed energy storage systems. IEEE Trans Power Syst 2013;28(4):3874–84.
[4] Zhang D, Li J, Hui D. Coordinated control for voltage regulation of distribution network voltage regulation by distributed energy storage systems. Protect Control Modern Power Syst 2018;3(1):1–8.
[5] Antoniadou-Plytaria KE, Kouveliotis-Lysikatos IN, Georgilakis PS, Hatziargyriou ND. Distributed and decentralized voltage control of smart distribution networks: models, methods, and future research. IEEE Trans Smart Grid 2017;8(6):2999–3008.
[6] Mokhtari G, Ghosh A, Nourbakhsh G, Ledwich G. Smart robust resources control in LV network to deal with voltage rise issue. IEEE Trans Sustain Energy 2013;4(4):1043–50.
[7] Demirok E, González P, Frederiksen KHB, Sera D, Rodriguez P, Teodorescu R. Local reactive power control methods for overvoltage prevention of distributed solar inverters in low-voltage grids. IEEE J Photovolt 2011;1:174–82.
[8] Turitsyn K, Šulc P, Backhaus S, Chertkov M. Options for control of reactive power by distributed photovoltaic generators. Proc IEEE 2011;99(6):1063–73.
[9] Calderaro V, Conio G, Galdi V, Piccolo A. Reactive power control for improving voltage profiles: a comparison between two decentralized approaches. Electr Power Syst Res 2012;83(1):247–54.
[10] Calderaro V, Conio G, Galdi V, Massa G, Piccolo A. Optimal decentralized voltage control for distribution systems with inverter-based distributed generators. IEEE Trans Power Syst 2014;29(1):230–41.
[11] Mahmud N, Zahedi A. Review of control strategies for voltage regulation of the smart distribution network with high penetration of renewable distributed generation. Renew Sustain Energy Rev 2016:582–95.
[12] Cheng L, Chang Y, Huang R. Mitigating voltage problem in distribution system with distributed solar generation using electric vehicles. IEEE Trans Sustain Energy 2015;6(4):1475–84.
[13] Kulmala A, Repo S, Jarventausta P. Coordinated voltage control in distribution networks including several distributed energy resources. IEEE Trans Smart Grid 2014;5(4):2010–20.
[14] Li P, Ji H, Wang C, Zhao J, Song G, Ding F, et al. A coordinated control method of voltage and reactive power for active distribution networks based on soft open point. IEEE Trans Sustain Energy 2017;8(4):1430–42.
[15] Agalgaonkar YP, Pal BC, Jabr RA. Distribution voltage control considering the impact of PV generation on tap changers and autonomous regulators. IEEE Trans Power Syst 2014;29(1):182–92.
[16] Weckx S, Gonzalez C, Driesen J. Combined central and local active and reactive power control of PV inverters. IEEE Trans Sustain Energy 2014;5(3):776–84.
[17] Valverde G, Van Cutsem T. Model predictive control of voltages in active distribution networks. IEEE Trans Smart Grid 2013;4(4):2152–61.
[18] Valverde G, Van Cutsem T. Control of dispersed generation to regulate distribution

and support transmission voltages. In: Proc IEEE PowerTech, Grenoble, France; 2013.
[19] Van Cutsem T, Valverde G. "Coordinated voltage control of distribution networks hosting dispersed generation. In: Proc international conference and exhibition on electricity distribution, Stockholm, Sweden; 2013.
[20] Bidgoli HS, Van Cutsem T. Combined local and centralized voltage control in active distribution networks. IEEE Trans Power Syst 2018;33(2):1374–84.
[21] Zheng Y, Hill DJ, Meng K, Hui SY. Critical bus voltage support in distribution systems with electric springs and responsibility sharing. IEEE Trans Power Syst 2017;32(5):3584–93.
[22] Yazdanian M, Mehrizi-Sani A. Distributed control techniques in microgrids. IEEE Trans Smart Grid 2014;5(6):2901–9.
[23] Robbins BA, Hadjicostis CN, Domínguez-García AD. A two-stage distributed architecture for voltage control in power distribution systems. IEEE Trans Power Syst 2012;28(2):1470–82.
[24] Zeraati M, Golshan ME, Guerrero JM. A consensus-based cooperative control of PEV battery and PV active power curtailment for voltage regulation in distribution networks. IEEE Trans Smart Grid 2019;10(1):670–80.
[25] Olivierx F, Aristidou P, Ernst D, Van Cutsem T. Active management of low-voltage networks for mitigating overvoltages due to photovoltaic units. IEEE Trans Smart Grid 2016;7(2):926–36.
[26] Wang Y, Tan KT, Peng XY, So PL. Coordinated control of distributed energy-storage systems for voltage regulation in distribution networks. IEEE Trans Power Del 2016;31(3):1132–41.
[27] Farag HE, El-Saadany EF, Seethapathy R. A two ways communication-based distributed control for voltage regulation in smart distribution feeders. IEEE Trans Smart Grid 2012;3(1):271–81.
[28] Farag HE, El-Saadany EF. A novel cooperative protocol for distributed voltage control in active distribution systems. IEEE Trans Power Syst 2013;28(2):1645–56.
[29] Robbins BA, Domínguez-García AD. Optimal reactive power dispatch for voltage regulation in unbalanced distribution systems. IEEE Trans Power Syst 2016;31(4):2903–13.
[30] Robbins BA, Zhu H, Domínguez-García AD. Optimal tap setting of voltage regulation transformers in unbalanced distribution systems. IEEE Trans Power Syst 2016;31(1):256–67.
[31] Šulc P, Backhaus S, Chertkov M. Optimal distributed control of reactive power via the alternating direction method of multipliers. IEEE Trans Energy Convers 2014;29(4):968–77.
[32] Liu HJ, Shi W, Zhu H. Distributed voltage control in distribution networks: online and robust implementations. IEEE Trans Smart Grid 2018;9(6):6106–17.
[33] Maknouninejad A, Zhihua Q. Realizing unified microgrid voltage profile and loss minimization: a cooperative distributed optimization and control approach. IEEE Trans Smart Grid 2014;5(4):1621–30.
[34] Utkarsh K, Trivedi A, Srinivasan D, Reindl T. A consensus-based distributed computational intelligence technique for real-time optimal control in smart distribution grids. IEEE Trans Emerg Top Comput Intell 2017;1(1):51–60.
[35] Yazdanian M, Mehrizi-Sani A. Distributed control techniques in microgrids. IEEE Trans Smart Grid 2014;5(6):2901–9.
[36] Mahmud N, Zahedi A. Review of control strategies for voltage regulation of the smart distribution network with high penetration of renewable distributed generation. Renew Sustain Energy Rev 2016;64:582–95.
[37] Aristidou P, Valverde G, Cutsem TV. Contribution of distribution network control to voltage stability: a case study. IEEE Trans Smart Grid 2017;8(1).
[38] Sun H, Guo Q, Zhang B, Guo Y, Li Z, Wang J. Master-slave-splitting based distributed global power flow method for integrated transmission and distribution analysis. IEEE Trans Smart Grid 2015;6(3):1484–92.
[39] Li Z, Guo Q, Sun H, Wang J, Xu Y, Fan M. A distributed transmission-distribution-coupled static voltage stability assessment method. IEEE Trans Power Syst 2018;33(3):2621–32.
[40] Guo Y, Gao H, Wu Q, Zhao H, Østergaard J, Mohammad S. Enhanced voltage control of VSC-HVDC connected offshore wind farms based on model predictive control. IEEE Trans Sustain Energy 2018;9(1):474–87.
[41] Behrangrad M. A review of demand side management business models in the electricity market. Renew Sustain Energy Rev 2015;47:70–83.
[42] Sugihara H, Yokoyama K, Saeki O, Tsuji K, Funaki T. Economic and efficient voltage management using customer-owned energy storage systems in a distribution network with high penetration of photovoltaic systems. IEEE Trans Power Syst 2013;28(1):102–11.
[43] Pasetti M, Rinaldi S, Manerba D. A virtual power plant architecture for the demand-side management of Smart Prosumers. Appl Sci 2018;8(3):1–20.
[44] Setlhaolo D, Xia X. Combined residential demand side management strategies with coordination and economic analysis. Int J Electr Power Energy Syst 2016;79:150–60.
[45] Olfati-Saber R, Murray RM. Consensus problems in networks of agents with switching topology and time-delays. IEEE Trans Autom Control 2004;49(9):1520–33.
[46] Camponogara E, Jia D, Krogh B, Talukdar S. Distributed model predictive control. IEEE Control Syst Mag 2002;22(1):44–52.
[47] Venkat A, Hiskens I, Rawlings J, Wright S. Distributed MPC strategies with application to power system automatic generation control. IEEE Trans Control Syst Technol 2008;16(6):1192–206.
[48] Shafiee Q, Stefanovic C, Dragicevic T, Popovski P, Vasquez JC, Guerrero JM. Robust networked control scheme for distributed secondary control of islanded microgrids. IEEE Trans Ind Electron 2014;61(10):5363–74.